Vietnam Journal of Science and Technology ***63*** *(2) (2025) 297-310*

doi:10.15625/2525-2518/18515

Preparation and characterization of lithium-stabilized coloidal silica as a silicate densifier for concrete surface treatment

Nguyen Hoang Thien Khoi[1, 2], Nguyen Ngoc Tri Huynh[1, 2], Huynh Ngoc Minh[1, 2], Nguyen Khanh Son[1, 2, *]

[1]*Faculty of Materials Technology, Ho Chi Minh City University of Technology (HCMUT), 268 Ly Thuong Kiet Street, District 10, Ho Chi Minh City, Viet Nam*

[2]*Vietnam National University Ho Chi Minh City, Linh Trung Ward, Thu Duc City, Ho Chi Minh City, Viet Nam*

[*]Emails: *ksnguyen@hcmut.edu.vn*

Received: 14 July 2023; Accepted for publication: 8 July 2024

Abstract. Enhancing the durability of concrete by safeguarding it against cracking and environmental deterioration is paramount. While silicate-based densifiers have been instrumental in shielding concrete surfaces from wear and environmental factors, the surging popularity of lithium silicate solutions faces a significant impediment due to the high cost of lithium, mainly attributed to its predominant use in manufacturing lithium batteries. To address this substantial challenge, an intriguing approach involves blending lithium silicate with colloidal silica, potentially offering a cost-effective and efficient solution for concrete surface treatment. This study delves into the feasibility of utilizing lithium-stabilized colloidal silica as a silicate densifier, focusing on their preparation, characterization, and efficacy in lab-scale applications. The results demonstrate that lithium-stabilized colloidal silica can heighten surface hardness while concurrently reducing porosity. However, it is worth noting that this approach presents particular challenges, particularly regarding preparation and water resistance, when compared to surfaces treated solely with lithium silicate. Addressing these hurdles holds promise for optimizing and enhancing lithium-stabilized colloidal silica and advancing the concrete surface treatment field in future research endeavours.

Keywords: silicate-based densifier, concrete hardener, lithium silicate hardener, colloidal silica, surface treatment.

Classification numbers: 2.9.2, 2.5.3.

1. INTRODUCTION

Concrete is widely used in civil engineering because of its strength, durability, and affordability. However, over time, concrete can crack and deteriorate, affecting its structural integrity and appearance. These issues stem from the hydration and hardening process of Portland cement, which produces heat and causes the mixture to set. During drying and contraction, internal stresses may lead to shrinkage and cracking. Early-age load bearing during

construction can also contribute to these problems. While reducing the water-cement ratio or adding reinforcement can help, these measures don't always fully prevent cracking.

Concrete cracking and deterioration can be severe, particularly in harsh environments like freeze-thaw cycles, moisture, and chemical attacks. Cracks can allow water and harmful agents to penetrate, leading to reinforcement corrosion, loss of strength, and surface spalling. Repairing damaged concrete is costly and time-consuming, requiring excavation, replacement, or strengthening. Thus, there is a need for effective solutions to prevent or mitigate this damage, such as surface treatments like silicate densifiers.[1].

Silicate-based densifiers have emerged as an alternative to polymer-based coatings for protecting concrete surfaces against environmental factors and wear [2]. These densifiers penetrate the concrete surface and chemically react with free lime to form a denser and more durable material, improving the concrete's strength, abrasion resistance, and overall performance [3]. The ion exchange reaction between the silicate solution $R_2O.SiO_2$ (where R is an alkaline ion, such as Na^+, K^+, or Li^+) and $Ca(OH)_2$ can be summarized as follows [4]:

$$R_2O.SiO_2 + Ca(OH)_2 + yH_2O \rightarrow xCaO.SiO_2.zH_2O + 2ROH + (x + y - x - 1)H_2O \quad (1)$$

The main product of the reaction is $xCaO.SiO_2.zH_2O$ (C-S-H) is the same mineral formed during cement hydration.

Lithium silicate (LiSi), a chemical compound produced through the fusion of lithium metal and silicate, exhibits considerable promise as an industrial material. It possesses remarkable properties such as abrasion resistance, waterproofing abilities, self-drying characteristics, fire resistance, resilience against adverse weather conditions, and non-toxicity. Due to its compatibility with reduced storage and usage requirements, LiSi has found extensive applications across various industries, including machinery manufacturing, maritime operations, ceramics production, and construction materials [5, 6]. Notably, this material has also made its way into the domain of road transportation. Innovatively, Gransberg and colleagues introduced a lithium-based hardening agent for concrete surface maintenance [7]. Their research unveiled that post-sandblasting treatment effectively mitigated wear and stripe marks, preserving slip resistance on road surfaces for up to three years. Subsequent investigations evaluated the abrasion resistance and gloss retention of limestone treated with lithium silicate, utilizing the AIMS system and Micro-Deval abrasion tests. The results demonstrated that chemical treatment bolstered the hardness and durability of fine particles while upholding angle and gloss resistance under abrasive conditions [8, 9]. Of particular note, the concurrent application of a LiSi hardener with sandblasting yielded intriguing outcomes. Sandblasting improved road surface porosity, enabling deeper penetration of the hardener, resulting in a tougher, more abrasion-resistant surface. Applying a LiSi hardener also maintained the structural integrity and form of the treated surface coating [10]. In summary, the literature above survey underscores the significant potential of LiSi in enhancing the abrasion resistance of limestone particles and improving the slip resistance of asphalt road surfaces. These benefits can be attributed to the outstanding properties of the resultant robust coating layer, characterized by superior abrasion resistance, waterproofing capabilities, self-drying attributes, and water insolubility. However, the widespread use of LiSi is constrained by the high cost of lithium, primarily due to its priority use in producing lithium batteries.

Developing colloidal silica or nano-silica (CoSi) has opened up new possibilities for concrete surface treatment. Bani Ardalan and colleagues conducted a study to investigate the effects of CoSi particles on concrete’s permeability and abrasion resistance by immersing concrete in a diluted CoSi solution. The results showed that maintaining concrete in a CoSi

adhesive solution resulted in lower permeability than in regular water [11]. In other words, CoSi hardening reduces the water permeability of concrete. Additionally, the study also indicated that different ratios of CoSi did not significantly affect the permeability of concrete [11]. Pengkun Hou and colleagues also studied the effectiveness and mechanisms of CoSi (with an average particle size of 10 nm) and its precursor, tetraethoxysilane (TEOS), in treating the surface of one-month-old cement mortar samples using brushing techniques [12]. The research showed that CoSi effectively reduced the water absorption ratio of cement mortar when sealed (with adhesive tape) at 50 °C. However, its effect at 20 °C was negligible, especially when maintained under unsealed conditions [12]. Pengkun Hou also studied CoSi and TEOS in the surface treatment of cement concrete, and the results demonstrated that CoSi and TEOS were effective in reducing water absorption and the water vapor transmission properties of concrete, especially in mixtures with a high water/cement ratio [12]. However, the main drawback of nano silica is its stability and ease of use on the construction site [13 - 15].

Combining LiSi and CoSi could offer an effective and cost-efficient solution for concrete surface treatment, enhancing performance and stability. This paper explores the potential of lithium-stabilized colloidal silica (LSCS) as a silicate densifier for concrete, providing a comprehensive analysis of its preparation, effectiveness, and potential drawbacks in real-world applications.

2. MATERIALS AND EXPERIMENTS

2.1. Materials

The LiSi used in our experiments was obtained from Simalco (Belgium) as a commercial product. It has a silicate modulus ranging from 3.5 to 4.8 and possesses desirable characteristics such as transparency and low viscosity. During the experiment of drying the solution in a laboratory oven at 60 °C until it reached a constant weight, it was observed that the solid component content was determined to be 24.63 %. Additionally, the pH of the solution was found to be 12.72 ± 0.01. This high alkaline property is considered an advantage of lithium-based hardeners over those based on sodium and potassium.

Colloidal silica, on the other hand, is a commercially available product from Allied High Tech Product that comprises a suspension of nano-sized silica particles with dispersants. Unlike LiSi, CoSi has an opaque white color and lower viscosity. The solid fraction content in the solution was measured to be 54.17 %, and the pH was recorded as 9.60 ± 0.01. This pH value indicates that the LiSi solution is more alkaline than the CoSi solution. According to literature studies, it is essential to maintain a pH range of 9 - 11 when working with silica to keep it in a stable colloidal state [16, 17]. This is valuable knowledge to keep in mind for any project involving silica to ensure success.

2.2. Preparation of LSCS solution

The LiSi solution was diluted with distilled water in a 1:1 weight ratio to create the mixture with CoSi. The solution was then stirred for an hour at room temperature using a magnetic stirrer. Subsequently, the CoSi solution was introduced to the diluted LiSi solution with varying weight ratios. It was gradually added while continuous stirring at around 1500 rpm and at a temperature of 50 °C. Figure 1 illustrates some critical steps in the process. As a result, different SiO_2 content in the prepared mixture solutions was achieved, ranging from 0.6 wt.% to 10 wt.% (Figure 2).

To ensure the stability of the CoSi material and prevent any adverse effects from exposure to air, the beaker container was covered during the 3 hours of stirring time. Following the process, the resulting solution exhibited an opaque white appearance, with the opacity varying depending on the silica content added. The solution was then stored in a sealed beaker for further material analysis and its subsequent use in coating concrete substrates. It is worth noting that these solutions demonstrated excellent stability and homogeneity, remaining unchanged even after several months of storage at room temperature. However, when the silica content in the mixed solution exceeds 5 wt.%, it may lead to instability and result in a milk-white appearance, potentially affecting the aesthetic aspect of the coating solution.

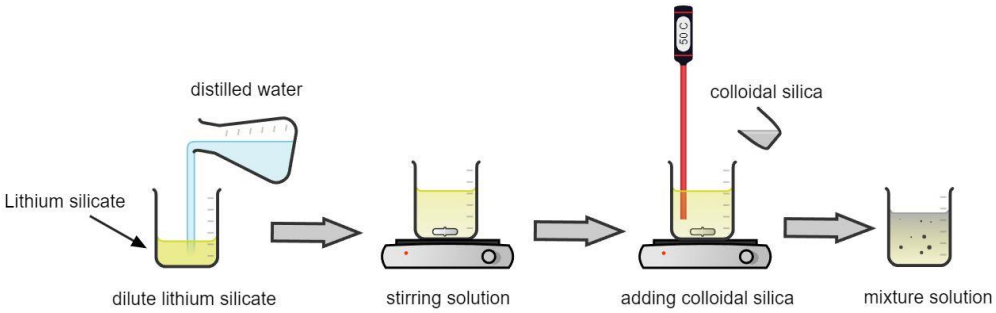

Figure 1. The main steps in processes of a LSCS synthesis.

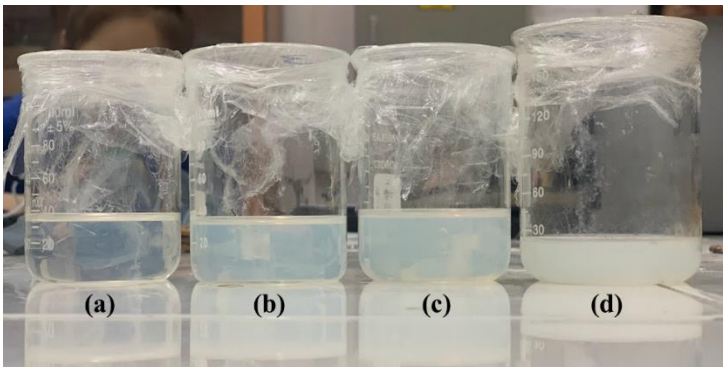

Figure 2. Prepared solution of LSCS with different weight ratios of SiO_2 (a) wt.%, (b) 3 wt.%, (c) 5 wt.% and (d) 10 wt.%.

2.3. Preparation of concrete surface and coating experiment

To prepare the concrete substrate for coating, raw materials were mixed to form cylindrical specimens (11.4 cm diameter, 20 cm height), consisting of Portland cement, river sand, crushed stone, and tap water. After 28 days of curing, the specimens were cut into 15 mm thick discs and ground using sandpaper (A180, P400, P800, P1000) to achieve a flat, defect-free surface. The grinding process reduced surface defects, resulting in a smoother finish. The next step involved applying a soft brush coating in two uniform layers to the disc samples, with each layer drying before the next was applied. The surface was divided into four regions for evaluation and comparison.

Figure 3 shows the surface differences in the cement-concrete samples before and after the grinding and washing process. It is apparent that the surface is flatter, and the number of surface defects has significantly decreased compared to the sample before grinding. However, it is worth

noting that the surface's dark areas, consisting of sand and stone aggregates, tend to be denser and less permeable to water than the surrounding cement mortar.

The next step involved the application of the soft brush coating method onto the concrete substrate. The surface of the disc sample was divided into four regions, as illustrated in Figure 4, for easy evaluation and comparison between different areas. The coating was consistently applied in two uniform layers, with the second layer being applied after the first had thoroughly dried to maintain homogeneity throughout the test.

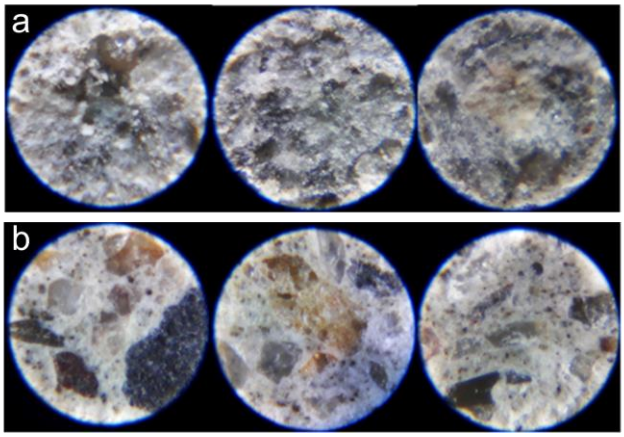

Figure 3. Optical microscope images (x250) of the sample surface before (a) and after (b) grinding process.

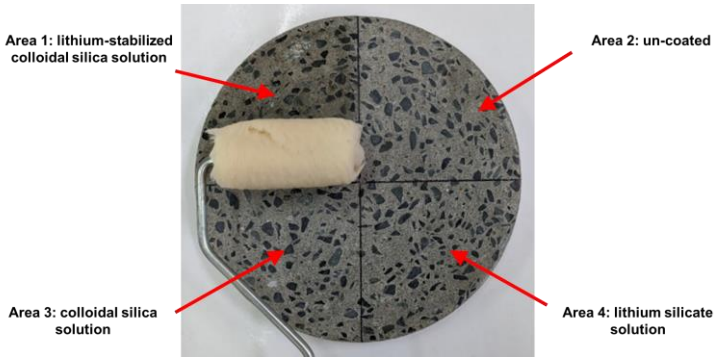

Figure 4. The concrete sample coated with three different silicate densifiers.

2.4. Characterization and test method

This study analyzed the FTIR spectra of prepared solutions within 400–4000 cm-1 using a NICOLET 6700 FT-IR Spectrometer (Thermo Fisher Scientific, USA) to examine their chemical characteristics. To assess particle size and dispersion stability in the coating solution, an LSCS solution with 10 wt.% silica was analyzed using Dynamic Light Scattering (DLS) and zeta-potential testing with the Horiba SZ-100V2 Instrument.

The study also examined coating morphology and microstructure using a Kyowa Me-Lux-3 optical microscope and a Hitachi S-4800 SEM. These instruments provided insight into the coatings' physical characteristics and structure. After a designated reaction period with the substrate, coated surfaces were evaluated for water absorption and hardness.

Water absorption was assessed using pedestal samples treated with different coating solutions. After curing for 7 days, samples were hermetically sealed with aluminum adhesive to ensure consistent coating thickness. They were then immersed in water up to half their thickness. After immersion for 1, 2, and 3 hours, samples were fractured at the central coated region to observe water ingress.

Surface scratch resistance was tested using the Mohs hardness test per ASTM C1895-20. A Mohs hardness pen at a 70-degree angle was used to create scratches, with progressively lower hardness pens applied until no scratching occurred. This method provided an accurate assessment of coating hardness

3. RESULTS AND DISCUSSION

3.1. Characterization of prepared solution of LSCS

Figure 5 displays the FTIR spectra of LiSi, CoSi, and four mixture solutions of LSCS (with different silica content) in the wavenumber range of 4000-400 cm^{-1}. The infrared spectrum of the LiSi solution reveals the presence of free H-O-H and O-H bonding in the range of 3650 to 3150 cm^{-1}, along with H-O-H bonds at 1638 cm^{-1}[18]. The 1037 cm^{-1} and 445 cm^{-1} peaks correspond to Si-O-Si oscillation [19, 20]. The characteristic Si=-O bond is also observed at a wave number of 1196 cm^{-1} [21]. In the infrared spectrum of the CoSi solution, the asymmetric stretching and shear bands of the Si–O–Si bonds are seen at 1093 cm^{-1}, while the symmetrical stretching vibrations of the Si=O bonds and the bending vibrations of the Si–O–Si bonds are observed at 801 and 469 cm^{-1}, respectively [21]. Moreover, a broad, intense absorption peak at 3420 cm^{-1} corresponds to the adsorbed water molecules [18].

The infrared spectra of the mixture solutions with silica content ranging from 0.6 wt.% to 10 wt.% show common peak positions in the range of 3650 to 3150 cm^{-1}, which are characterized by the H-O-H and free O-H bonds, along with the appearance of the H-O-H bond at 1638.0 cm^{-1} [18]. The Si-O-Si bond appears at around 1037 cm^{-1} in all spectrums [21]. Additionally, the Si=O bond appears at 773.3 cm^{-1}, and the Si-O-Si bond appears at 445 cm^{-1} [21].

Based on the FTIR analysis results, it can be inferred that the mixture of CoSi and LiSi exhibits characteristic peaks such as Si-O-Si and H-O-H bonds. The mixing process of the two solutions does not indicate the appearance of new bonds, and the solution is homogeneous with good dispersion of the components. The obtained spectra demonstrate an average transmission of the mixed spectra of the two raw components, reflecting the mixture ratio.

Figure 6 depicts the particle size distribution of a LSCS solution containing 10 wt.% silica contents. The analysis results indicate that the particle sizes range from 50.53 nm to 193.48 nm, with an average particle size of 88.6 nm. This average size slightly increases compared to the average particle size of the CoSi material, typically 75 nm. However, the size distribution spectrum overall exhibits good concentration (Figure 6-a). The increase in silica particle size at the nanoscale may be attributed to emulsion flocculation. Agglomeration is a common phenomenon observed in colloidal solutions, where small particles come into contact and adhere to one another, forming larger clusters. Agglomeration can be influenced by particle concentration, pH, temperature, and stabilizing agents [22, 23].

Additionally, the zeta surface potential measurement method was employed to investigate the stability of the emulsion solution. The zeta potential pattern of the solution sample displays a peak potential at -6.2 mV (Figure 6-b). Comparing this value to the range of potential values associated with solution stability, it can be concluded that the synthesized solution exhibits relatively stable characteristics. This observation aligns with the visual assessment of the solution, as shown in Figure 2.

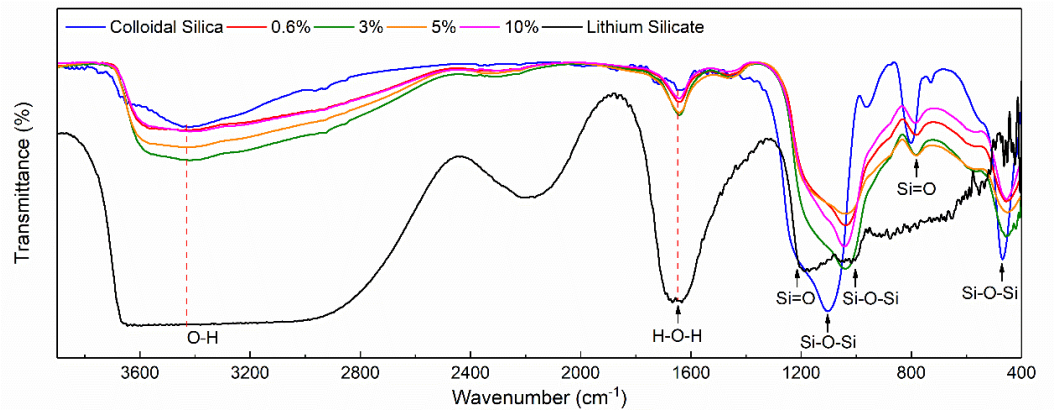

Figure 5. FTIR spectra of various concrete densifiers including: LiSi solution, CoSi and prepared solution of LSCS.

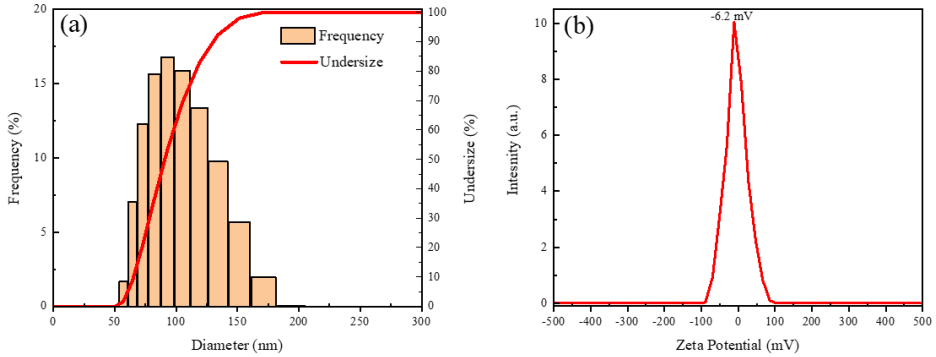

Figure 6. (a) Particle size distribution result; (b) Pattern of zeta potential of the solution of LSCS with 10 wt.% silica.

3.2. Precipitation reaction between silicate densifier solutions and $Ca(OH)_2$

Figure 7 illustrates the experimental process of monitoring the reaction between the coating solutions and $Ca(OH)_2$. The results showed that adding LiSi to $Ca(OH)_2$ resulted in the formation of a white precipitate at room temperature, which increased in amount over time at 1 day, 3 days, and 7 days. This suggests that the reaction between LiSi and $Ca(OH)_2$ was ongoing and that the precipitate continued to form as time progressed and the presence of a high concentration of Ca^{2+}.

In contrast, adding $Ca(OH)_2$ to the CoSi solution caused the immediate destabilization of the CoSi solution, leading to agglomeration and settling of nano-silica particles to the bottom of the beaker. The settled precipitate made it challenging to observe the amount formed accurately. However, gradually clarifying the solution above the settled portion was observed over time. This hindered the ability to determine the appropriate amount of CoSi for the reaction, posing

difficulties in the application process. The loss of stability of CoSi when added to the $Ca(OH)_2$ solution is in line with previous research, where the ion composition and concentration of the surrounding environment of the nano-silica particles cause instability of the CoSi solution [24]. The presence of one-valence and two-valence ions, such as calcium (Ca^{2+}), changes the ion charge of the silica sol and leads to two agglomeration mechanisms. The first mechanism reduces the electrostatic repulsion force between the nano silica particles, making the attractive force dominant. Additionally, these ions can bridge between the nano-silica particles, neutralizing positions on the silica surface and forming physical bridges between two silica particles if their charge-neutral surfaces collide and coordinate with the water oxygens binding to the surfaces [24].

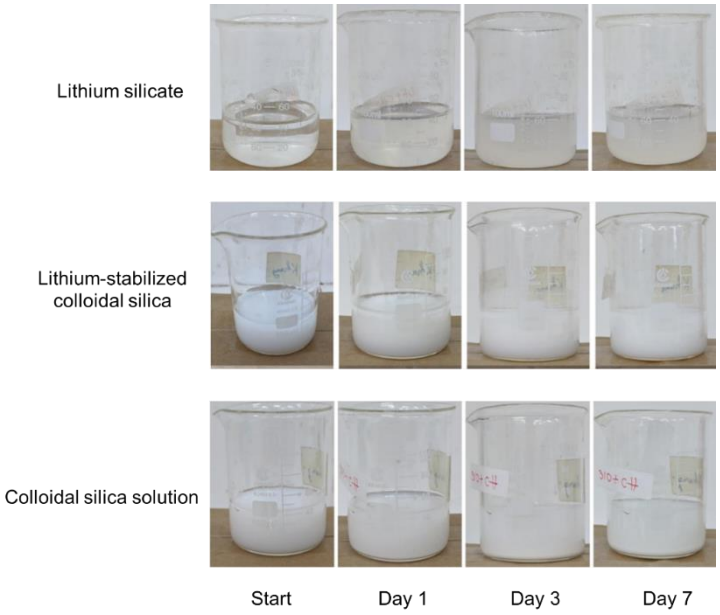

Figure 7. Monitoring the progress of precipitation reaction between silicate densifier solutions and $Ca(OH)_2$.

In the LSCS solution, a white precipitate initially formed and later settled due to the high pH of $Ca(OH)_2$, disrupting the non-agglomeration equilibrium. However, when applied to cement-concrete, the lower $Ca(OH)_2$ concentration slows mineral precipitation, occurring gradually rather than as immediate agglomeration, as seen with CoSi.

In this study, the reactivity of a $Ca(OH)_2$ solution with various silicate solutions was rigorously investigated by monitoring pH values within reaction samples over three distinct time intervals: one day, three days, and seven days, as presented in Figure 8. The objective was to understand how these solutions interacted chemically and how their pH levels evolved. Upon conducting a one-day observation, it was observed that the pH values of the LiSi and CoSi solutions exhibited a slight decrease. This initial change in pH suggested the formation of acidic products resulting from the reactions. However, the pH value of the LSCS solution remained notably stable at approximately 11.83 during this brief timeframe, indicating that this particular solution did not yield acidic products within the early stages of the reaction.

Over three days, the pH of all solutions declined, indicating ongoing chemical reactions. LiSi and CoSi solutions showed a more significant drop to 10.05 and 10.39, respectively, suggesting increased acidic product formation, while LSCS remained relatively stable at 11.50.

After seven days, this trend continued, with LiSi and CoSi dropping further to 10.01 and 10.37, while LSCS slightly decreased to 11.48. These results highlight the interaction between $Ca(OH)_2$ and silicate solutions, leading to reduced alkalinity. LiSi showed the most pronounced pH drop, while CoSi maintained a higher pH than its original state, indicating differences in reaction products. This study enhances understanding of the pH dynamics in these chemical systems.

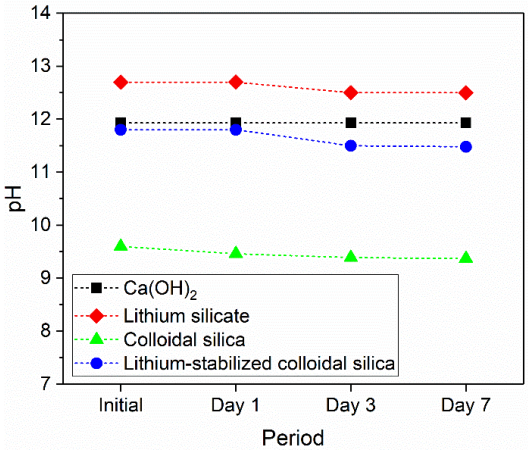

Figure 8. pH values of reaction solutions with $Ca(OH)_2$ at 1 day, 3 days, and 7 days intervals.

The higher pH value observed in the LSCS solution compared to the LiSi and CoSi solutions can be elucidated by the stabilizing influence of lithium ions on CoSi particles [25]. The CoSi particles inherently possess a high surface area and a propensity to undergo aggregation, leading to instability and a concurrent decrease in pH value. However, introducing lithium ions into the LSCS solution is pivotal in mitigating this aggregation phenomenon. Lithium ions exhibit a capacity to interact with the surface of CoSi particles, forming a protective layer that acts as a barrier against aggregation. This protective layer maintains the stability of the CoSi solution [25]. As a result, the LSCS solution exhibits a higher pH value than the LiSi and CoSi solutions, both lacking this stabilizing effect [25]. Therefore, the elevated pH value observed in the LSCS solution can be primarily attributed to lithium ions, which contribute significantly to stabilizing CoSi particles. This stabilization effect is crucial in maintaining the solution's pH level and preventing the formation of acidic products, as observed in the experimental results.

3.3. Characterization of coated concrete sample

3.3.1. Visualization by optical microscope

The optical microscope images in Figure 9 provide a detailed view of the surface morphology of different coating layers on the sample. By comparing the uncoated and coated samples, it can be observed that the coating layers effectively filled the surface defects, such as pores and cracks, resulting in a smoother surface. This could be attributed to the materials in the coating layer that could penetrate and fill in the pores and cracks, leading to a more uniform surface.

The coating layers show significant color variation. The transparency of the LiSi coating makes it ideal for preserving the original material's color and texture, while the milky white

CoSi coating suggests the presence of nano-silica particles. The LSCS coating appears less milky than CoSi, offering a more natural look. Adhesion is also crucial; LiSi and LSCS coatings adhered well to aggregate surfaces, enhancing protection. In contrast, the CoSi coating covered both aggregate and cement mortar but formed overlapping, non-continuous scales, potentially weakening adhesion. The LSCS coating's smaller, less dense scales suggest better adhesion and protection than CoSi.

3.3.2. Morphological analysis by SEM

Figure 10 shows SEM images of surfaces coated with LiSi, CoSi, and LSCS solutions. The uncoated concrete surface had loosely arranged C-S-H minerals with visible pores, increasing corrosion and degradation risks.

The LiSi-coated surface formed a dense, continuous layer, filling pores and strengthening the microstructure through strong bonding. After 14 days, rod-shaped C-S-H minerals and hexagonal $Ca(OH)_2$ plates developed, enhancing strength and adhesion. The LSCS coating improved microstructure with thin rod-like C-S-H minerals, while the CoSi coating, though uneven, also formed C-S-H and $Ca(OH)_2$ minerals, indicating bonding with the concrete.

Overall, coated surfaces were more compact than uncoated ones, showing product layer deposition and microstructure alteration. $Ca(OH)_2$ minerals were present, and reactions with the coating may continue under favorable conditions. These results highlight the coatings' effectiveness in enhancing concrete durability and performance.

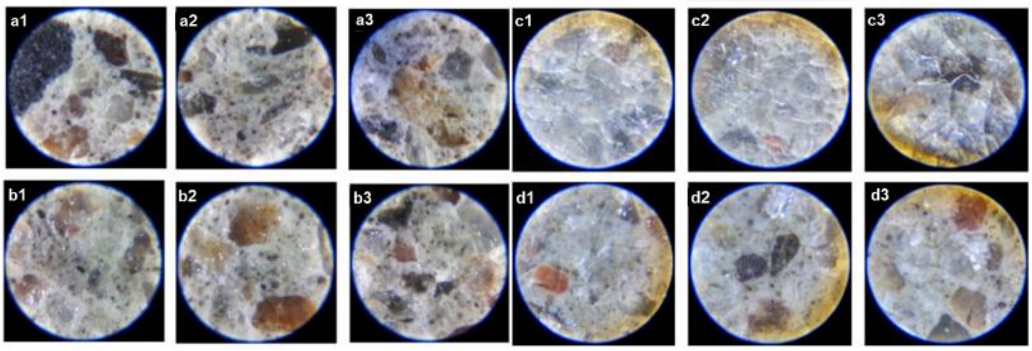

Figure 9. Optical microscope images (x250) of the sample surface of (a1) – (a3) uncoating area, (b1) – (b3) area coated with LiSi, (c1) – (c3) area coated with CoSi, and (d1) – (d3) area coated with LSCS (d) after 14 days.

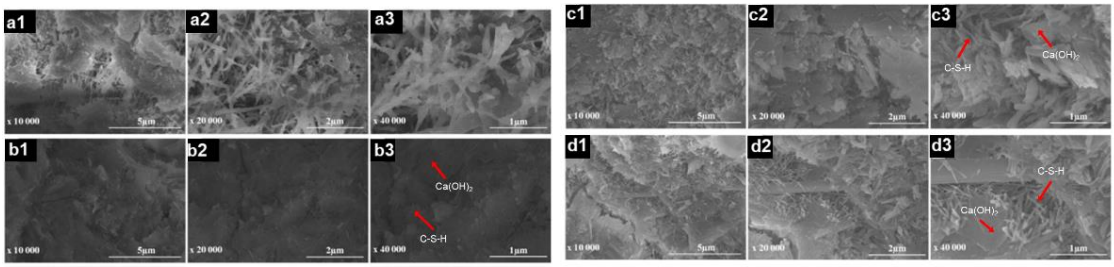

Figure 10. SEM images of the sample surface of (a1) – (a3) uncoating area, (b1) – (b3) area coated with LiSi, (c1) – (c3) area coated with CoSi, and (d1) – (d3) area coated with LSCS after 14 days.

3.3.3. Water absorption

Figure 11 depicts the depth of water penetration through various sample areas at 1, 2, and 3 hours after immersion. Upon immersion of the concrete sample in water for 1 hour, it was observed that water had penetrated all areas of the sample, including the areas coated with the LSCS, CoSi, and LiSi solutions, as well as the uncovered areas. The thickness of water penetration in the uncovered area was significantly higher than that of the coated areas, indicating that the water resistance of the coated areas was superior under the same experimental conditions. The consistency of the results obtained from points equidistant from the sample surface in contact with water further validated the reliability of the findings.

After 2–3 hours of immersion, water penetration thickness in LSCS- and CoSi-coated areas was similar, while LiSi-coated areas showed lower penetration, indicating superior water resistance. This suggests LiSi has better permeability and reactivity than CoSi. Figure 9 analysis further revealed that CoSi and LSCS coatings formed flaky layers, whereas LiSi created a continuous layer, likely contributing to the observed differences in water resistance.

3.3.4. Scratch resistance (Mohs hardness)

Table 1 presents the results of the surface hardness measurements of concrete samples coated with three solutions: LiSi, CoSi, and LSCS, as measured by the Mohs scale after 14 and 21 days of coating. Using a Mohs pen allowed the hardness of the samples at various positions to be measured, thereby evaluating the effect of the testing pen on the coating layer. The presented hardness values indicate the relative hardness between different coated areas, which provides insight into the effectiveness of the coating layer on the concrete surface over time.

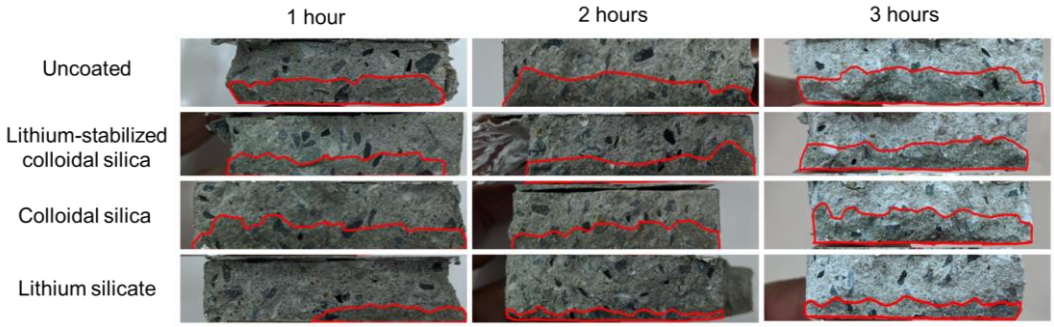

Figure 11. Water absorption rate through different sample areas at time intervals of 1, 2, and 3 hours after immersion.

Table 1. Surface hardness of coatings according to Mohs scale at 14 and 21-day intervals.

Time of reaction	**Hardness level in Mohs scale**		
	LiSi	*CoSi*	*LSCS*
7-day	5.5	3.5	5.5
21-day	6.5	4.0	6

After 7 days, the surface hardness of LSCS and LiSi-coated areas reached 5.5, while CoSi-coated areas had a lower hardness of 3.5. By 21 days, LiSi increased to 6.5, LSCS to 6, and CoSi to 4. This indicates that surface hardness improves over time due to increased density and

reaction. However, CoSi consistently showed lower hardness, suggesting weaker reactivity with concrete. These findings emphasize the need to assess coating performance over time to determine effectiveness.

4. CONCLUSIONS

In conclusion, the experimental results show that a mixture of CoSi and LiSi (up to 10 wt.% silica) demonstrates promising characteristics. The mixture is homogeneous, with well-dispersed components, as confirmed by FTIR and particle size analysis. Upon reacting with $Ca(OH)_2$, the LSCS solution forms a crystallized product. Microscope and SEM images reveal that LSCS creates a smooth, continuous surface on concrete, enhancing its appearance and hiding cracks. Over 7 and 21 days, the surface hardness of the coated concrete increases, showing improved durability. The LSCS also offers better water resistance compared to uncoated concrete, though not as much as pure LiSi. This two-component mixture appears to be a cost-effective alternative to traditional LiSi, but further research is needed to optimize its effectiveness for concrete applications.

Acknowledgements. Corresponding author would like to thank DECOCRETE Co. Ltd. for materials support; facility for Mohs hardness test and Ho Chi Minh city University of Technology, VNU HCM for supporting this study.

Credit authorship contribution statement. Nguyen Hoang Thien Khoi: Investigation, Manuscript preparation. Nguyen Ngoc Tri Huynh: Formal analysis. Huynh Ngoc Minh: Formal analysis. Nguyen Khanh Son: Manuscript revision, Methodology, Supervision.

Declaration of competing interest. The authors declare that they have no known competing financial interests or personal relationships that could have appeared to influence the work reported in this paper.

REFERENCES

1. Neville A. M., Brooks J. J. - Concrete technology, Longman Scientific & Technical, England, 1987.
2. Pan X., Shi Z., Shi C., Ling T. C., Li N. - A review on concrete surface treatment Part I: Types and mechanisms, Constr. Build. Mater. **132** (2017) 578-590. https://doi.org/10.1016/j.conbuildmat.2016.12.025.
3. Kim J., Kitagaki R. - Behavior of hydrates in cement paste reacted with silicate-based impregnant, Cem. Concr. Compos. **114** (2020) 103810. https://doi.org/10.1016/j.cemconcomp.2020.103810.
4. Provis J. L., Van Deventer J. S. - Alkali activated materials: state-of-the-art report, Springer Science & Business Media, Germany, 2013.
5. Kato Y., Someya N. - Effect of silicate-based surface penetrant on concrete durability, in: Grantham M., Muhammed Basheer P. A., Magee B. and Soutsos M. (Eds.), Concrete Solution, Taylor & Francis Group, London, 2014, pp. 393-397.
6. Hazehara H., Soeda M., Hashimoto S. - Fundamental study on characteristics of silicate based surface penetrants and effects of improvement on concrete structures, in: Furuta H., Frangopol D. and Akiyama M. (Eds.) , Life-Cycle of Structural Systems: Design, Assessment, Maintenance and Management, CRC Press, London, 2014, pp. 971-978.

7. Gransberg D. D., Pittenger D. M. - Maintaining Airport Pavement Friction Using Surface Densification, Proceedings of the 9th International Conference on Managing Pavement Assets, Vol. 9, Washington, 2015, pp. 300-309.
8. Zhang H., Zhang Z., Lv J., Zhang G. - Effect of Lithium Silicate–Impregnated Limestone Aggregate on Skid Resistance Properties of Bituminous Mixture, J. Mater. Civ. Eng. **34** (2022) 04022251. https://doi.org/10.1061/(ASCE)MT.1943-5533.0004409.
9. Zhang Z., Zhang H., Lv J., Li W. - Performance evaluation of skid-resistant surface treatment using lithium silicate for limestone bituminous pavement, Constr. Build. Mater. **342** (2022) 127990. https://doi.org/10.1016/j.conbuildmat.2022.127990.
10. Lv J., Wang R. - Literature Review of Shot Blasting and Lithium Silicate Treatment to Improve the Anti-sliding Performance of Asphalt Pavement, Proceedings of the 5th International Conference on Information Science, Computer Technology and Transportation, Vol. 5, Shenyang, 2020, pp. 662-666.
11. Ardalan R. B., Jamshidi N., Arabameri H., Joshaghani A., Mehrinejad M., Sharafi P. - Enhancing the permeability and abrasion resistance of concrete using colloidal nano-SiO_2 oxide and spraying nanosilicon practices, Constr. Build. Mater. **146** (2017) 128-135. https://doi.org/10.1016/j.conbuildmat.2017.04.078.
12. Hou P., Cheng X., Qian J., Shah S. P. - Effects and mechanisms of surface treatment of hardened cement-based materials with colloidal nanoSiO2 and its precursor, Constr. Build. Mater. **53** (2014) 66-73. https://doi.org/10.1016/j.conbuildmat.2013.11.062.
13. Jalal M., Mansouri E., Sharifipour M., Pouladkhan A. R. - Mechanical, rheological, durability and microstructural properties of high performance self-compacting concrete containing SiO2 micro and nanoparticles, Mater. Des. **34** (2012) 389-400. https://doi.org/10.1016/j.matdes.2011.08.037.
14. Ji T. - Preliminary study on the water permeability and microstructure of concrete incorporating nano-SiO_2, Cem. Concr. Res. **35** (2005) 1943-1947. https://doi.org/10.1016/j.cemconres.2005.07.004.
15. Land G., Stephan D. - The influence of nano-silica on the hydration of ordinary Portland cement, J. Mater. Sci. **47** (2012) 1011-1017. https://doi.org/10.1007/s10853-011-5881-1.
16. Gu S., Shi Y., Wang L., Liu W., Song Z. J. C., Science P. - Study on the stability of modified colloidal silica with polymer in aqueous environment, Colloid Polym. Sci. **292** (2014) 267-273. https://doi.org/10.1007/s00396-013-3109-4.
17. Chung I., Kim T., Kang J., Tan M. M., Dung N. T. K., Huynh M. D., Dai Lam T., Chinh N. T., Giang B. L., Hoang T. J. C., Physicochemical S. A., Aspects E. - Preparation, stabilization and characterization of 3-(methacryloyloxy) propyl trimethoxy silane modified colloidal nanosilica particles, Colloids Surf. A **585** (2020) 124066. https://doi.org/10.1016/j.colsurfa.2019.124066.
18. Kloprogge J. - Application of vibrational spectroscopy in clay minerals synthesis, Dev. Clay. Sci. **8** (2017) 222-287. https://doi.org/10.1016/B978-0-08-100355-8.00008-4.
19. Dorosz D., Zmojda J., Kochanowicz M. - Investigation on broadband near-infrared emission in Yb^{3+}/Ho^{3+} co-doped antimony–silicate glass and optical fiber, Opt. Mater. **35** (2013) 2577-2580. https://doi.org/10.1016/j.optmat.2013.07.022.
20. Ivanov V. G., Reyes B. A., Fritsch E., Faulques E. - Vibrational states in opals revisited, J. Phys. Chem. C **115** (2011) 11968-11975. https://doi.org/10.1021/jp2027115.

21. Khan R., Khare P., Baruah B. P., Hazarika A. K., Dey N. C. - Spectroscopic, kinetic studies of polyaniline-flyash composite, Adv. Chem. Engineer. Sci. **1** (2011) 37-44. https://doi:10.4236/aces.2011.12007.
22. Zeng N., Zhao H., Liu Y., Wang C., Luo C., Wang W., Ma T. - Optimizing of the colloidal dispersity of silica nanoparticle slurries for chemical mechanical polishing, Silicon **14** (2022) 7473–7481. https://doi.org/10.1007/s12633-021-01448-y.
23. Becit B., Duchstein P., Zahn D. - Molecular mechanisms of mesoporous silica formation from colloid solution: Ripening-reactions arrest hollow network structures, PLoS ONE **14** (3) e0212731. https://doi.org/10.1371/journal.pone.0212731.
24. Hendrix D., McKeon J., Wille K. - Behavior of colloidal nanosilica in an ultrahigh performance concrete environment using dynamic light scattering, Materials **12** (2019) 1976. https://doi.org/10.3390/ma12121976
25. da Cruz Schneid A., Albuquerque L. J. C., Mondo G. B., Ceolin M., Picco A. S., Cardoso M. B. - Colloidal stability and degradability of silica nanoparticles in biological fluids: A review, J. Sol-Gel Sci. Technol. **102** (2022) 41-62. https://doi.org/10.1007/s10971-021-05695-8.